ORIGINAL RESEARCH PAPER

CrossMark

An adjusted design approach for concentrically braced frames in low-to-moderate seismicity areas

Alper Kanyilmaz[1] (ORCID) · **Hervé Degée[2]** · **Carlo Andrea Castiglioni[1]**

Abstract
Steel concentrically braced frame (CBF) configuration is a common construction application in Europe. In the low-to-moderate seismicity context, European building codes provide two alternative design methods for CBFs; engineers have to choose between a "non-dissipative" method (DCL) neglecting all seismic provisions, and a "dissipative" one (DCM), applying its complex and expensive ductility requirements. Currently, the preferred method is the former one, because of its simplicity. Such a choice may lead on one side to oversized profiles that are unduly expensive, on the other side to possibly unsafe solutions due to the unpredictable nature of the regions characterized by low-to-moderate seismicity, where rare but strong earthquakes are foreseeable. On the other hand, enforcing engineers to apply strict "high-dissipative" rules seems too conservative for this case, which would result in over-safe, but uneconomic structures. This article proposes an adjusted design approach for the low-to-moderate seismicity design of CBF structures, aiming to satisfy both economy and safety criteria. The proposed approach is based on the exploitation of the three features of CBF systems, which have not been deeply investigated so far: "frame action provided by gusset plates", "contribution of compression diagonal and its post-buckling strength and stiffness", and "energy dissipation capacity of non-ductile bracing joint connections". The paper investigates these aspects by means of incremental dynamic analysis of case studies, based on the numerical models calibrated on full-scale experimental tests published elsewhere by the authors. As a result, it provides design recommendations and presents economic comparisons between the buildings designed with current Eurocode approach and the proposed one.

Keywords Low-to-moderate seismicity · Concentrically braced frames · Frame action · Compression diagonal · Bracing joints · Preloaded bolts

✉ Alper Kanyilmaz
  alper.kanyilmaz@polimi.it

[1] Department of Architecture, Built Environment and Construction Engineering, Politecnico di Milano, Milano, Italy

[2] Hasselt University, Hasselt, Belgium

1 Introduction

The main idea of the traditional seismic design philosophy is to provide the structure with a global inelastic behaviour (i.e. globally and homogenously distributed damage) during a strong earthquake event (Degée et al. 2018; EN1998-1-1 2005). Regarding seismic design, a wide knowledge has been already gained from the numerous research activities focusing on the performance of the structures under strong ground motions. This resulted in quite advanced provisions regarding the high seismicity design in Europe (EN1998-1-1 2005; NTC 2008). Therefore, where "high-seismicity" is concerned, practising engineers have clear indications, as well as a solid experience in the field. On the other hand, using the provisions tuned for high seismicity, is neither feasible nor economic in the case of design in the "low-to-moderate seismicity" context. Research is needed to identify specific methods to build safe and economic structures in low-to-moderate seismicity zones.

In Eurocodes, reference design acceleration is associated with a probability of exceedance of a certain ground motion, during the service life of the structure. In this framework, low-to-moderate seismicity hazard can be defined as the probability of occurrence of an earthquake in a specific region, characterized by a magnitude, duration and number of high amplitude cycles clearly lower than a high-seismicity hazard (Gioncu and Mazzolani 2014). Within the European context, this can be translated into an upper bound of peak ground acceleration (PGA) value combined with a specific response spectrum type (Type 2 for low-to-moderate seismicity), considering a short duration event. In this article, "low-to-moderate" seismicity is defined based on a reference PGA on stiff soil equal to, or lower than 0.15 g with a reference return period of 475 years, which is compatible with EN1998-1-1 provisions (2005).

In European codes (EN1998-1-1 2005) three ductility classes are proposed for the design of steel structures. They are called "DCL" (ductility class low), "DCM" (ductility class medium), and "DCH" (ductility class high). Both DCH and DCM require the application of capacity design rules and SC2 execution criteria (EN 1090-2 2011) with significant costs for manufacturing and quality control, while DCL design refers only to the EN1993 (2005) without requiring any ductility rules along with SC1 execution criteria. Concerning low-to-moderate seismicity zones, the current version of Eurocodes allows building designers to choose between DCL and DCM. DCM has a much higher reliability and safety level but leads to a significant increase in the structure costs. On the other hand, DCL is economic but highly unreliable since it does not require seismic protection measures (Table 1). The general tendency of engineers is often to choose the DCL approach because of its simplicity. Therefore, the current European approach for low-to-moderate

Table 1 Advantages and disadvantages of DCL and DCM approaches

	High dissipative design (DCM or DCH)	Low dissipative design (DCL)
Pros	1. Reduced steel tonnage 2. Reduced foundation costs	1. Reduced design effort 2. Simple connection details, easier fabrication 3. Reduced errors in design and fabrication
Cons	1. Complex and costly detailing requirements (usually omitted by designers)	1. Less reliable performance 2. Uneconomic

seismicity design should be adjusted to have a good balance between safety and economy with the help of specific rules compatible with the target seismicity level.

Gioncu and Mazzolani (2014) in their book "Seismic Design of Steel Structures", dedicated an entire section to "Low-to-Moderate Seismic Regions". They explain the main issues regarding the seismic design in these areas, which include the characteristics of low-to-moderate ground motions and related structural design problems. Kelly and Zona (2006) highlight the fact that in the United States, building designers and constructors based in moderate seismicity areas do not have extensive experience with earthquake-resistant construction, and pointed out that the consequence of misusing complicated seismic provisions could result in unsafe and unnecessarily costly buildings. Their article covers topics that include determining site class and seismic design category, selecting a steel seismic-force-resisting system, and applying detailing requirements according to the American standards. Murty and Malik (2008) raises the challenges in the current design practice in the large low-to-moderate seismicity regions of India, where over the last decade, there has been a sudden surge in the construction activity. Among their proposals for the future are the new design strategies implementing an awareness campaign for all stakeholders, and updating seismic design provisions towards improving earthquake safety in the low-to-moderate seismicity zones.

The necessity to treat low-to-moderate seismicity in a different manner is valid in general, for all construction types in the world, and underlined by several researchers (Gioncu and Mazzolani 2014; Kelly and Zona 2006; Murty and Malik 2008; Nordenson and Bell 2000; Mayer Rosa 1993; Pinto 2000). This article focuses on steel Concentrically Braced Frame (CBF) systems, being a very popular steel structure type in the European construction industry (Degée et al. 2018). In seismic regions, CBF systems must be designed in a way that the diagonal elements (bracings) should yield first before any damage to the beams, columns and connections. To meet this general requirement, several seismic design practices are adopted around the world (Elghazouli 2009; Landolfo 2012; Costanzo et al. 2017; Brandonisio et al. 2012; Tremblay 2002; Tremblay et al. 2003; Longo et al. 2008; Kazemzadeh Azad et al. 2017; Shen et al. 2017). US codes classify CBFs in two categories as special concentrically braced frames (SCBF) and ordinary concentrically braced frames (OCBF) (American Institute of Steel Construction 2010). SCBFs are designed with high response modification factors (corresponding to the European "behaviour factor") and strict detailing requirements, and OCBFs are designed with small response modification factors and simpler detailing requirements. European standards classify CBF structures according to three ductility categories: DCL, DCM and DCH. Both US and European standards rely only on the bracings for the resistance, ductility and energy dissipation. In Japan, braced structures are designed taking into account the moment resisting beam-end connections as a back-up against bracing post failure strength and stiffness, and global ductility parameters take into account directly the ductility provided by the frame action, and compression bracings. This is a totally different approach from current European design practice (Marino et al. 2005), where the frame action and compression bracings are not even taken into account.

Several researchers studied the CBFs in the context of low-to-moderate seismicity. Available studies in this context include the research done by Bradley et al. (2017) who proposed a seismic design philosophy for low-ductility structures in moderate seismicity regions, exploiting the reserve capacity and elastic flexibility of CBFs, by Aboosaber and Hines (2011) who found that the semi-rigid joints of the secondary moment resisting frame can prevent a sidesway collapse, when the primary lateral force resisting system (bracings) is significantly damaged, and by Stoakes (2012) who identified the contribution of the

flexural capacity of several beam-to-column connection types to the seismic performance of CBFs. Yet, there is not sufficient experimental evidence to characterize the ductility, resistance and stiffness resources of full-scale global CBFs in the low-to-moderate seismicity context. There are three main topics which are not dealt in detail in the current European seismic codes, which constitute the core subjects of this article:

- Contribution of the frame action provided by the gusset plate connections to the global CBF behaviour.
- Contribution of the compression diagonal, and its post-buckling strength and stiffness to the global CBF behaviour.
- Energy dissipation resources of the non-ductile bracing joints including slippage and plastic ovalization in bolted bracing connections.

These are the potential structural resources of CBFs that are commonly not considered in the design, due to insufficient experimental evidence and knowledge. This article investigates the contribution of these phenomena to the seismic performance of steel CBF structures designed for low-to-moderate seismicity, by means of incremental dynamic numerical simulations performed with the models calibrated on the full-scale experimental tests. Furthermore, it suggests adjustments to the current Eurocode design recommendations, and presents economic comparisons between the buildings designed with current Eurocode approach and the adjusted one.

2 Experimental background

Within MEAKADO research project (Degée et al. 2018), a set of full-scale tests have been performed, which focused on the structural characteristics of 36 CBF specimens designed for low-to-moderate seismicity according to EN1993 recommendations (EN 1993-1-1 2005). Several aspects of the test program and detailed results have been recently published elsewhere (Kanyilmaz 2017a, b, 2018). In this article, a summary of the results is given to set a base for the numerical calibration and parametric studies. The dimensions of the test specimens correspond to the full size of a one-story frame (with 2.6 m height and 4.3 m length) extracted from a multi-story CBF, adjusted according to the capacity of the testing facilities. Cyclic tests have been performed using bracing profiles with three different cross sections to investigate and quantify the following phenomena:

1. Contribution of the frame action provided by the gusset plate connections to the global CBF behaviour (Kanyilmaz 2017a).
2. Contribution of compression diagonal, and its post-buckling strength and stiffness to the global CBF behaviour (Kanyilmaz 2017b).
3. Energy dissipation resources of non-ductile bracing joints including bolt slippage and plastic ovalization in bolted bracing connections (Kanyilmaz 2018).

To study these phenomena, the specimens are assembled with different configurations (X-braced, single braced, without bracings, with and without gusset plates), inside a moment resisting test frame (MRF), and an ideally pinned test frame (PC).

2.1 Contribution of the frame action provided by the gusset plate connections to the global CBF behaviour

Full-scale tests (Fig. 1) (Kanyilmaz 2017a) have clearly shown that the gusset plate connections are a substantial resource of additional stiffness and strength. Even in the cases where the bracings completely failed, the frame action provides consistent stiffness, strength and hysteresis input until large inter-storey drifts. In particular, following quantifications have been made:

- The main components of the frame action were gusset plates (Fig. 1b). At 2% inter-storey drift, 75% of the elastic stiffness and 79% of the ultimate resistance sources were the gusset plate connections. The remaining part was due to the beam-to-column shear connections.
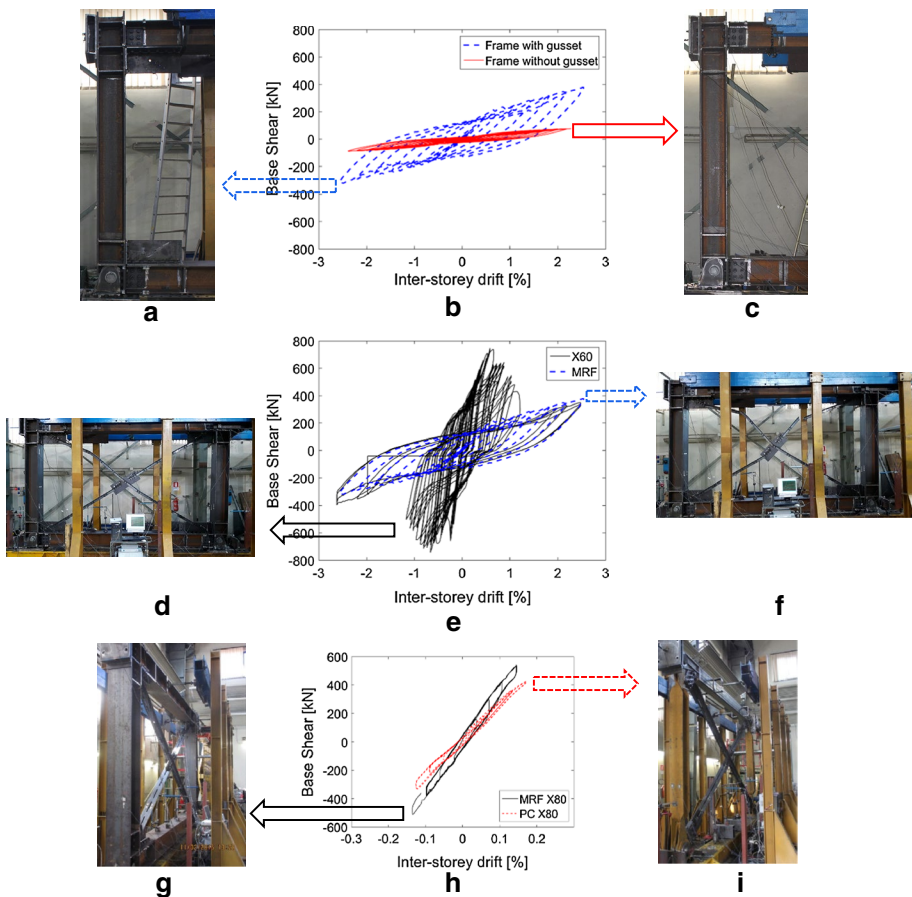

Fig. 1 Test summary focusing on secondary frame action. Detailed information is published in Kanyilmaz (2017). **a** Frame with gusset, **b** comparison of the global behaviour, **c** frame without gusset, **d** X-braced frame, **e** comparison of the global behaviour, **f** X-braced frame with fully collapsed bracings, **g** X-braced "MRF" specimen, **h** comparison of the initial stiffnesses and **i** X-braced "PC" specimen

- Secondary frame resistance (including the frame action and the post-buckling resistance of the diagonals) ranged between 58 and 80% of the overall specimen resistance (depending on the bracing configuration).
- After the total failure of bracings, at collapse limit state (2% inter-storey drift), secondary frame action provided more than 46% of the resistance previously developed by the overall braced specimen (Fig. 1e).
- The overall ductility of the test specimens was much higher when the frame ductility was taken into account. The additional ductility was due to the "frame reserve ductility", and counted between 1.7 and 4.9 times the ductility provided by bracings alone.
- The frame action contributed to the lateral stiffness by a percentage ranging between 7.6 and 13.5%, which depended on the structural configuration, and bracing sections.
- The global initial stiffness of the PC specimens was lower with respect to MRF specimens, with the same bracing profiles. This difference is caused by different boundary conditions of two specimen types (Fig. 1h).
- The positive effect of the secondary frame action was more significant in the case of the test specimens with more slender diagonals.

2.2 Contribution of compression diagonal, and its post-buckling strength and stiffness to the global CBF behaviour

3 types of bracing profiles and 6 different configurations have been tested with different slenderness values and boundary conditions (ideally pinned bracing ends and standard connections). Structural behaviour of the specimens with and without a compression diagonal was considerably different. Major experimental findings are listed hereafter (Fig. 2) (Kanyilmaz 2017b):

- Contribution of the compression diagonal to the global stiffness ranged between 38.4 and 54.2%.
- Minimum global resistance provided by the compressed bracings during post-buckling stage was between 16 and 32% of the specimens' overall global elastic resistance. The percentage increased with decreasing bracing slenderness.
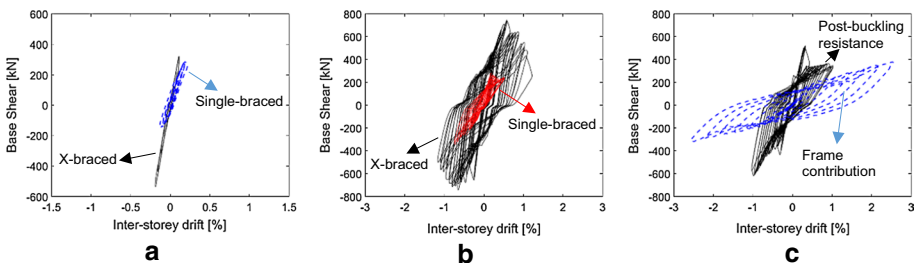

Fig. 2 Summary of the tests with a focus on the contribution of compression diagonal. Detailed information is published elsewhere (Kanyilmaz 2017b). **a** X-braced vs single-braced specimens, initial stiffness comparison (bracing profile 2L60x8, MRF test), **b** X-braced vs single-braced specimens global behaviour comparison (bracing profile 2L60x8, MRF test) and **c** The post-buckling capacity of a single-braced specimen (single bracing configuration with profile 2L80x8, MRF test)

- After net section fractures initiated, bracings provided an extra strength under compression forces. Thanks to cyclic crack closure, after net section fracture, the contribution of the diagonal in compression to the overall resistance was 18 and 23%, for two of the specimens which had net section fractures.
- Global resistance of the X-braced specimen during the post-buckling stage ranged between 47 and 82% of its global elastic resistance, depending on the bracing cross-section.
- A larger global ductility was obtained, when the inelastic deformation was far from the bolt holes during post-buckling. This could only be achieved in case of 2L80x8 (least slender) bracing profiles, due to their larger cross-section that is less penalized by the bolt holes.
- Global ductility of the specimen with the strongest bracings was the highest of all.
- Braced MRF specimens had three plastic hinges; one at the middle, and two at both ends of the bracings, while PC specimens had one plastic hinge only in the middle. The difference was due to the rotation demand provided by the semi-rigid beam-to-column connections of MRF specimens, while the bracing ends were hinged in PC specimens.
- It has been observed that the plastic buckling predictions calculated by EN1993-1-1 (2005) are very different from the experimental results, when effective length factors are assumed according to the code recommendations.

2.3 Energy dissipation resources of non-ductile bracing joint connections

Full-scale test results (Kanyilmaz 2018) showed that non-ductile slip-resistant joints have a noteworthy capacity to dissipate seismic energy, in terms of yielding at bolt holes due to bearing and friction caused by the slippage of preloaded bolts. The quantified overall joint ductility ranged between 2.8 and 7.9. Between 30 and 59% of the overall joint ductility was provided by the slippage of bolts. Moreover, the block tearing resistance of the joints were larger by up to 65% with respect to the code estimations. These test results showed the capacity of non-ductile joints to dissipate seismic energy in terms of yielding at bolt holes due to bearing and friction caused by the slippage of preloaded bolts, which may be valuable for the low-to-moderate seismicity actions (Fig. 3).

3 Numerical calibration

Even such a large testing program summarized in the previous section is not sufficient to provide general design recommendations, because the test specimens were a representation of a single floor and bay, and the dynamic response was not investigated. In order to generalize the experimental results, a numerical study has been conducted to investigate the performance of multi-story frames under dynamic actions. The numerical models have been validated on the results of the full-scale tests summarized in the previous section. With these validated models, the performance of a multi-story building case study has been investigated by means of incremental dynamic analysis method (Vamvatsikos and Cornell 2002), based on low-to-moderate earthquake ground motions. Finally, based on the experimental and numerical studies, recommendations have been provided for the design of CBF structures in low-to-moderate seismicity.
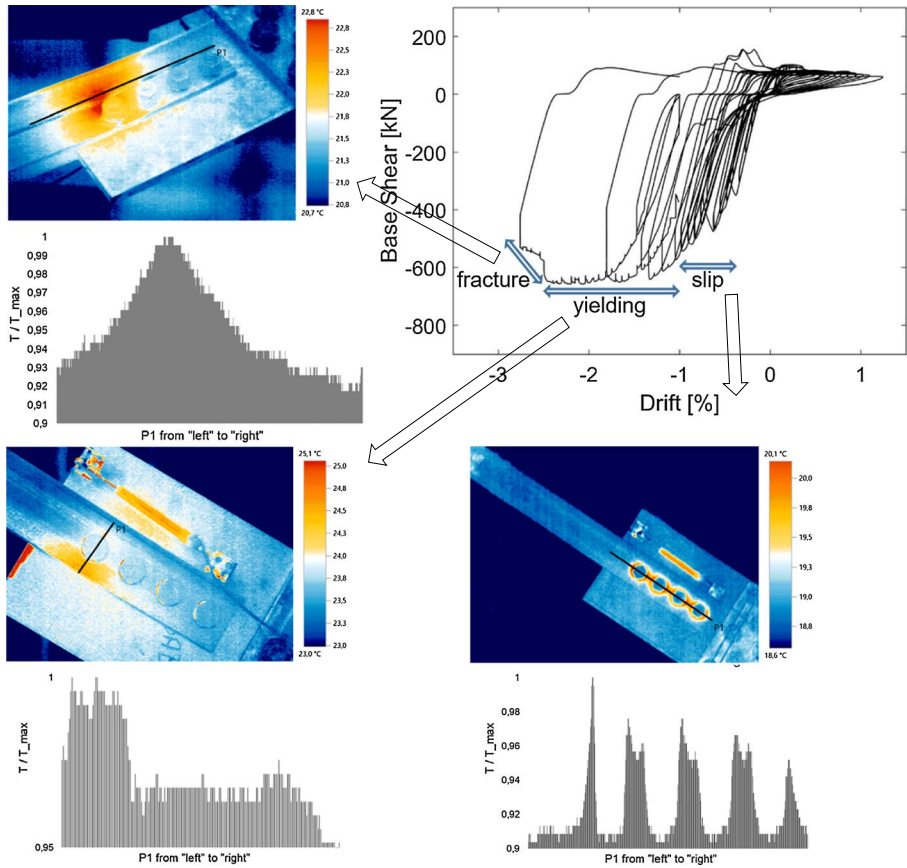
Fig. 3 Tests summary focusing on bracing joint behaviour (Histograms show the normalized temperature (T/T_max) values along the line P1 drawn on the images). Detailed information is published in Kanyilmaz (2018)

All structural components have been modelled with fiber-based distributed plasticity approach (Uriz and Mahin 2008; Sabelli 2001; Kanyilmaz 2015a; Kanyilmaz and Castiglioni 2015; Kanyilmaz et al. 2015). A nonlinear stress–strain relationship with kinematic hardening has been adopted. Beam element stiffness and length are updated during the nonlinear analysis. A numerical sensitivity analysis has been performed to validate the suitability of fiber-based distributed plasticity modelling approach to simulate the inelastic cyclic response of bracing elements, and to define the optimized number of fiber elements and integration points in the profiles. These sensitivity simulations were based on previous experimental data from the literature, and have already been published by the authors (Kanyilmaz 2015b). However, none of the tests taken from literature had "inelastic" resources that can be valuable for low-to-moderate seismicity regions (such as bracing bolt hole ovalizations and slippage, and flexural stiffness and plasticity provided by the gusset plate connections. Therefore, in this section, the calibration of the numerical models has been presented, where these parameters have been also introduced by means of

axial and flexural nonlinear spring elements thanks to the experimental results presented in the previous section.

The calibration study has been performed as follows:

1. In order to simulate the ovalization of bolt holes and slippage in bolted connections, nonlinear axial springs formulated in MEAKADO project (Degée et al. 2018; Martin et al. 2017) have been validated on PC specimen test results. The formulation of these "equivalent models" is based on a component method procedure (Eurocode 3: Design of Steel Structures—Part 1–8: Design of Joints 2005) and takes into account slippage and hole ovalizations by means of elasto-plastic spring elements working in parallel. With this procedure, a nonlinear axial force–displacement curve has been obtained for the test specimens.

2. In order to take into account the contribution of the flexural behaviour of the frame connections, an analytical procedure developed elsewhere (Stoakes 2012) has been adopted for the beam-to-column gusset plate connections of the test frames. With this procedure, initial and ultimate flexural stiffness and the strength of beam-to-column connections involving gusset plate are estimated analytically for positive and negative bending, and then validated with experimental results.

3. Parameters obtained from points (1) and (2) have been adopted in the simulation of single bracing MRF specimens. At this point, a full calibration has been obtained.
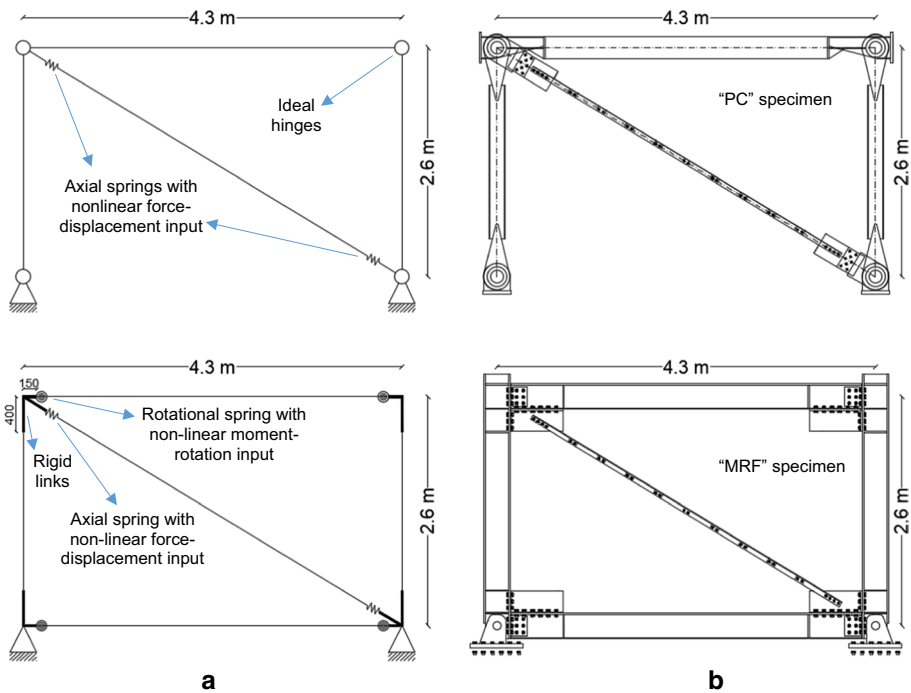

Fig. 4 Numerical simulation characteristics of the single diagonal PC and MRF specimens. **a** Numerical models and **b** test specimen configuration
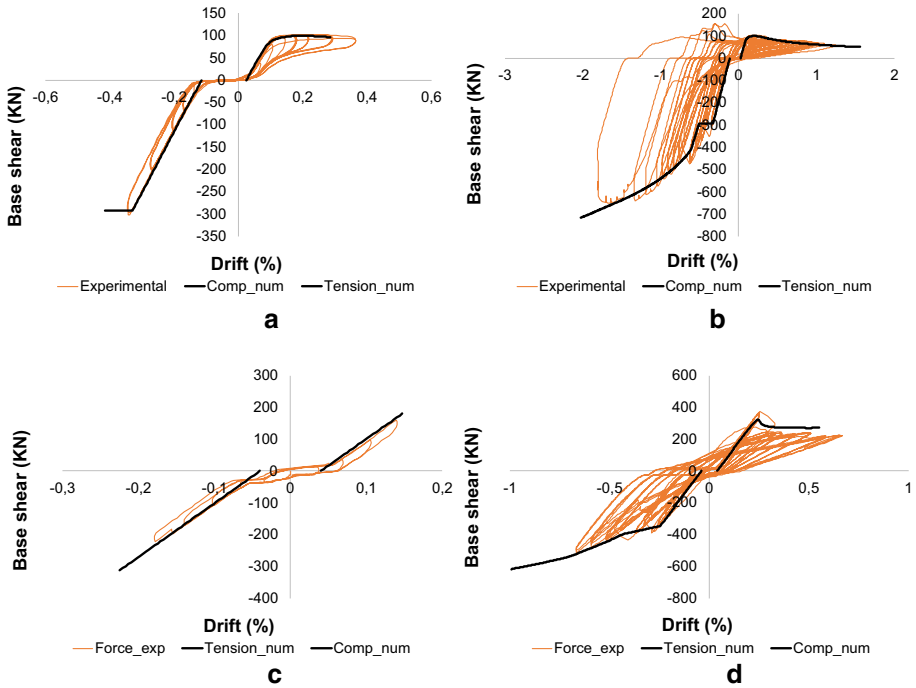
Fig. 5 Back-bone curves constructed on the experimental results. **a** S80-PC Initial stiffness comparison, **b** S80-PC Global behavior comparison, **c** S70-MRF Initial stiffness comparison and **d** S70-MRF Global behaviour comparison

Table 2 Comparison between numerical and experimental results	S80-PC		S70-MRF	
	Exp.	Num.	Exp.	Num.
K_{ie} (KN/int. drift)	1201	1300	1775	1679
F_{ty} (KN)	471	415	431	395
F_{cy} (KN)	97	94	376	310
F_{ts} (KN)	346	293	381	346
F_{tu} (KN)	654	664	N.A.	617
F_{cu} (KN)	60	55	235	270

Figure 4 shows the equivalent springs used for PC and MRF specimens. Both frame types have the same overall dimensions, but differ in their boundary conditions. For PC specimen, rotational degrees of freedom are released to represent the ideal hinged connections obtained during the tests. In both cases, the columns are restrained at their base against horizontal and vertical displacement with hinges. An initial imperfection of L/750 has been introduced to the bracings.

The model has been calibrated with reference to the specimens S80-PC and S70-MRF. Based on the experimental results, back-bone curves have been constructed,

which indicate a very good correlation between numerical and experimental results in terms of initial stiffness, global resistance under tension and compression forces, and global cyclic behaviour (Fig. 5).

Initial elastic stiffness (K_{ie}), global tension (F_{ty}) and compression (F_{cy}) yielding, slippage under tension (F_{ts}), and global ultimate tension (F_{tu}) and compression (F_{cu}) capacities obtained by the numerical simulations and corresponding experimental results are reported in Table 2.

4 Case study

The overall objective of the case study is to measure the impact of the experimental findings inside a realistic multi-story building example under earthquake actions. This will bring into light the inherent dissipative capacity of low-ductility braced frames, which can be economically useful to consider in low-to-moderate seismicity regions. For this reason, four different cases have been analysed based on the same structural configuration. First, a benchmark has been developed using the common analysis procedures of current practice, neglecting the frame action provided by the gusset plate connections. This benchmark is called "DCL". Then, three new models have been developed upon this benchmark, each one having a different parameter that is set to simulate different aspects of CBFs such as nonlinear behaviour of the connections, bracing profile slenderness and joint ductility. The seismic performance of each case has been quantified by means of incremental dynamic analysis.

4.1 Building models

Building models are based on a CBF system designed within MEAKADO research project (Degée et al. 2018). Preliminary numerical analysis performed on 4, 6, 8, and 12-floor buildings have shown that 4-floor configuration was the most vulnerable one under low-to-moderate seismicity actions. Thus, a 4-story CBF with N-bracing configuration has been chosen as a benchmark (Fig. 6b).
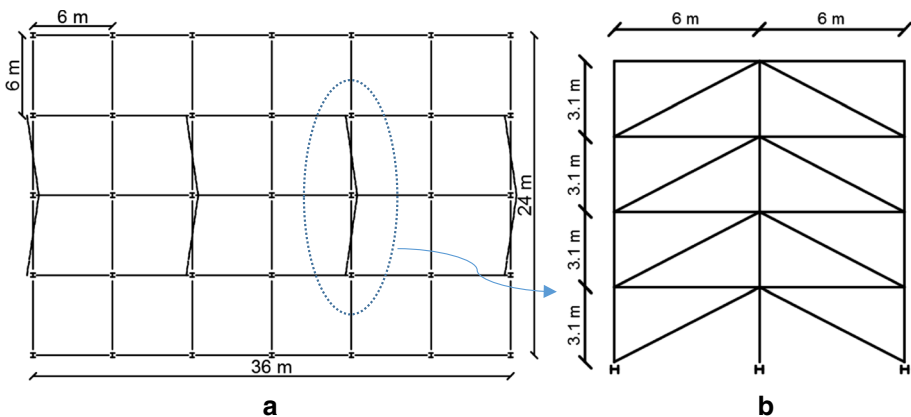

Fig. 6 Benchmark frame geometry under investigation. **a** Building plan and **b** CBF under investigation

4170 Bulletin of Earthquake Engineering (2018) 16:4159–4189

Table 3 Frame parameters

Story height	3.10 m
Span length	6.00 m
Bracing clear length	6.75 m
Steel material	S275
Elastic modulus of steel	210,000 MPa
Dynamic mass at each floor	151,200 kg
Dynamic mass at last floor	75,600 kg
Column profiles	HEB300
Beam profiles	HEA300

This model represents one of the four identical vertical plans of stability of a CBF building regular in plan and elevation (Fig. 6a). It has been designed according to low-ductility (DCL) concept of EN1998-1-1 (2005) for low-to-moderate seismicity actions, hence the stringent requirements regarding the bracing slenderness, joint over-strength ("capacity design"), and global over-strength homogeneity have been fully disregarded. Spectrum type II has been considered with a PGA of 0.15 g, and soil type B. Behaviour factor has been set to q = 1.50. The steel profiles and connection details are kept similar to the ones experimentally tested, so that reliable results can be obtained from calibrated numerical models. Model parameters are shown in Table 3.

Bracing member sizes and relevant design parameters are shown in Table 4. Since the over-strength homogeneity rule and the slenderness limits [prescribed by EN1998-1 (2005)] are violated on purpose, same bracing profiles have been used for all the floors. This solution is the "cheapest" for design and fabrication purposes, but critical for a "soft story" collapse mechanism. Therefore, it represents a "worst case" scenario in terms of safety, for a building designed according to low-dissipative design criteria for low-to-moderate seismicity regions.

This benchmark model is called as "DCL". It has been analysed by standard modelling assumptions with pinned joints at both bracing and beam ends. Other 3 models have been developed upon this benchmark, each one taking into account an extra characteristic of the benchmark frame, calibrated from the experimental findings of this study, i.e. nonlinear rotational hinges at beam ends, decreased compression diagonal slenderness, and increased joint ductility. The benchmark model also includes joint nonlinearity, which avoids overestimating the plastic capacity of the bracings that are not designed according to dissipative capacity design rules.

With reference to Table 5, the modelling assumptions of different cases can be summarized as:

Table 4 Bracing configuration of benchmark model DCL

Floor no.	Bracing profile	Non-dimensional slenderness	Over-strength ratio
4	2L70x7	3.25	2.44
3	2L70x7	3.25	1.86
2	2L70x7	3.25	1.34
1	2L70x7	3.25	1.12
		λ_{max}: 3.25 ($\gg$ 2.00)	Ω_3/Ω_1: 1.66 ($\gg$ 1.25)

🖉 Springer

Table 5 Different modelling assumptions used in the analysis of case studies

Design		Analysis model
	Action	Design assumption	
DCL	EC8 type 2 spectrum	EC8 DCL design (resulting diagonal slenderness = 3,25)	Hinged beam-column connections
DCL+1	PGA = 0,15 g	EC8 DCL design (resulting diagonal slenderness = 3,25)	Actual beam-column connections
DCL+2	soil type: B	EC8 DCL design with additional limitation on the diagonal slenderness ($\bar{\lambda}_{max} = 2.25$)	Actual beam-column connections
DCL+3	q = 1,50	EC8 DCL design with additional limitation on the diagonal slenderness ($\bar{\lambda}_{max} = 2.25$) and capacity design of the joints	Actual beam-column connections

- All 4 configurations have been designed for the same seismic action (i.e. response spectrum type II, PGA = 0,15 g, soil type B, q = 1,5).
- DCL and DCL + 1 are characterized exactly by the same design.
- DCL + 2 is a classical DCL design with additional limitation on the maximum slenderness of the bracing diagonals $(\bar{\lambda}_{\max} = 2.25)$.
- DCL + 3 is a classical DCL design with additional limitation on the maximum slenderness of the bracing diagonals $(\bar{\lambda}_{max} = 2.25)$ and capacity design of the bracing connections.
- Analysis is carried out according to the following assumptions: DCL is modelled assuming hinged beam-column connections, while DCL + 1 to DCL + 3 are modelled taking explicitly into account the actual stiffness and strength of the beam-column connections with the presence of the gusset plate.

Nonlinear behaviour of the CBF connections has been simulated by means of elasto-plastic spring elements and rigid links (Fig. 7). The role of each element is described hereafter:

- *Nonlinear joint spring (J1, J2)*: Simulates the nonlinear behaviour of the pre-loaded bracing joints, caused by the ovalization of bolt holes and slippage of bolts.
- *Nonlinear rotational spring*: Simulates the nonlinear rotational behaviour of beam-to-column joints with gusset plates.
- *Rigid links*: Simulate the offsets induced by gusset plates to the connections.

The input parameters of each nonlinear spring have been calculated with the analytical models described and calibrated in the previous section. Essential model inputs are summarized in Table 6, where:

|	
$R_{el,avg}$	Rotational spring elastic stiffness (average of positive and negative stiffness)
$R_{pl,avg}$	Rotational spring plastic stiffness (average of positive and negative stiffness)
λ	Diagonal non-dimensional slenderness
J_{ini}	Initial joint stiffness
J_{pl}	Plastic joint stiffness
$N_{j,s}$	Slip joint resistance
$N_{j,u}$	Ultimate joint resistance
C_R	Capacity design ratio ($N_{j,u}/1.1 * Y_{Rd} * N_{pl,Rd}$, where Y_{Rd}: 1.00)
$N_{pl,Rd}$	Tensile plastic resistance of the diagonal element
Y_{Rd}	Over-strength parameter
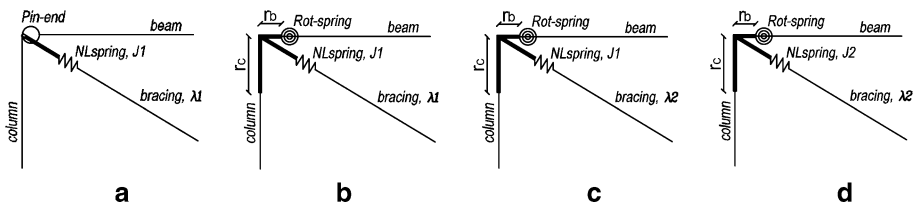
Fig. 7 Modelling parameters. **a** DCL, **b** DCL + 1, **c** DCL + 2 and **d** DCL + 3

Table 6 Values of modelling parameters

	$R_{el,avg}$ (KNm/rad)	$R_{pl,avg}$ (KNm/rad)	λ	J_{ini} (kN/mm)	$N_{j,s}$ (kN)	J_{pl} (kN/mm)	$N_{j,u}$ (kN)	$N_{pl,Rd}$ (kN)	C_R
DCL	0 (Pinned)	0 (Pinned)	3.25	1772	343	153	434	512	0.77
DCL+1	22,338	6057	3.25	1772	343	153	434	512	0.77
DCL+2	22,338	6057	2.25	1883	343	209	760	845	0.82
DCL+3	22,338	6057	2.25	1883	343	209	1162	845	1.25

Fig. 8 Bracing joint behaviour compared with bracing tensile resistance for all models
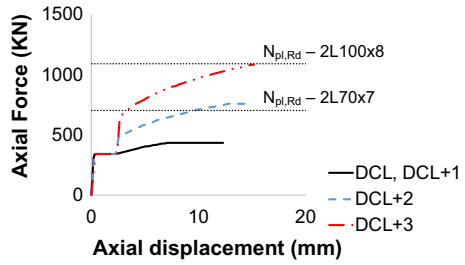
Since the nominal material properties have been used in the numerical models, material over-strength factor γ_{Rd} is taken as 1.0 in the calculation of the C_R parameter. Experimental studies have shown that the failure mode was always due to the net section capacity of the double-angle bolted joints, therefore C_R, in this case, has been calculated based on the design net section resistance of the joint considering the nominal material strength.

It can be seen that DCL + 2 has a less slender diagonal but a similar capacity design ratio with the first two models ($C_R < 1$). DCL + 3 has the same diagonal with DCL + 2, moreover, it meets the capacity design requirement ($C_R = 1.25 > 1$). The axial force–displacement behaviour of the bracing joint spring elements has been shown in Fig. 8, where their slip and ultimate resistances are compared with the tensile plastic resistance of the bracing of the relevant model ($N_{pl,Rd}$).

Numerical models have been developed and analysed using Strand7 nonlinear finite element analysis software (2014). Modelling procedure has been defined after an extensive sensitivity analysis investigating the effects of boundary conditions, imperfections, material and geometrical nonlinearity, and damping parameters published elsewhere (Kanyilmaz 2015a; Kanyilmaz et al. 2015). Columns are continuous along the frame height, and they are designed to be part of the vertical resisting system. All beams, bracings and columns have been modelled using the fiber-based distributed plasticity approach (Kanyilmaz 2015b). A discrete meshing is applied for the finite element model, which was optimized during the numerical sensitivity analysis. Local buckling and low-cycle fatigue effects have been kept beyond the scope of this study, since the behaviour of moderately slender bracings is not strongly influenced by such phenomena. Three fundamental mode values of all models are reported in Table 7. Adding each "+", the model becomes stiffer except for the DCL + 3 where the only modification was introduced in terms of the ductility of bracing connection.

Table 7 Modal information for different models

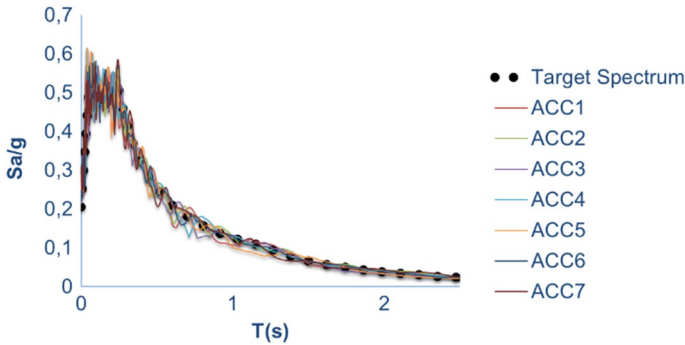| Model	1st natural mode (s)	Mass participation of 1st mode (%)	2nd natural mode (s)	Mass participation of 2nd mode (%)	3rd natural mode (s)	Mass participation of 3rd mode (%)
DCL	0.61	88	0.21	9	0.13	2
DCL + 1	0.57	88	0.20	9	0.13	2
DCL + 2	0.47	87	0.16	10	0.11	3
DCL + 3	0.47	87	0.16	10	0.11	3

Fig. 9 Response spectrum of 7 accelerograms compared with the target spectrum

Table 8 Scale factors used in incremental dynamic analysis

Scale factor	PGA (g)	PoE in 50 years (%)	Return Period (T_R)
0.33	0.049	63	50
0.56	0.084	39	101
1.00	0.150	10	475
1.26	0.189	5	975
1.65	0.248	2	2475
2.00	0.300		
2.50	0.375		
3.00	0.450		
4.00	0.600		
5.00	0.750		

4.2 Nonlinear dynamic time-history analysis

Global ductility and collapse resistance of the models have been estimated by means of incremental nonlinear dynamic acceleration time-history simulations (Vamvatsikos and Cornell 2002). Due to the limited database of the low-to-moderate ground motions, seven artificial time history accelerograms have been created according to the target design response spectrum, which have a duration of 10 s. Since the magnitude correlates quite well with the duration that is quite short in case of low-to-moderate seismicity (just a few seconds), the slightly overestimated duration in the time-histories (stationary part taken equal to 10 s as suggested in EN1998-1-1) partly compensates the lack of variability that would be possessed by natural time histories. Type 2 design spectrum has been constructed according to EN1998-1-1 (2005), considering a probability of exceedance of 10% in 50 years with a PGA of 0.15 g and assuming soil type B (S = 1.35). Figure 9 shows the response spectrum of chosen accelerograms (ACC1 to ACC7) compared to the target design spectrum.

In the simulations, 2% Rayleigh damping has been used. As described in Table 8, the PGA has been incremented gradually until the global collapse of structures took place. Each increment is described by a "scale factor". Five of these factors were compatible with
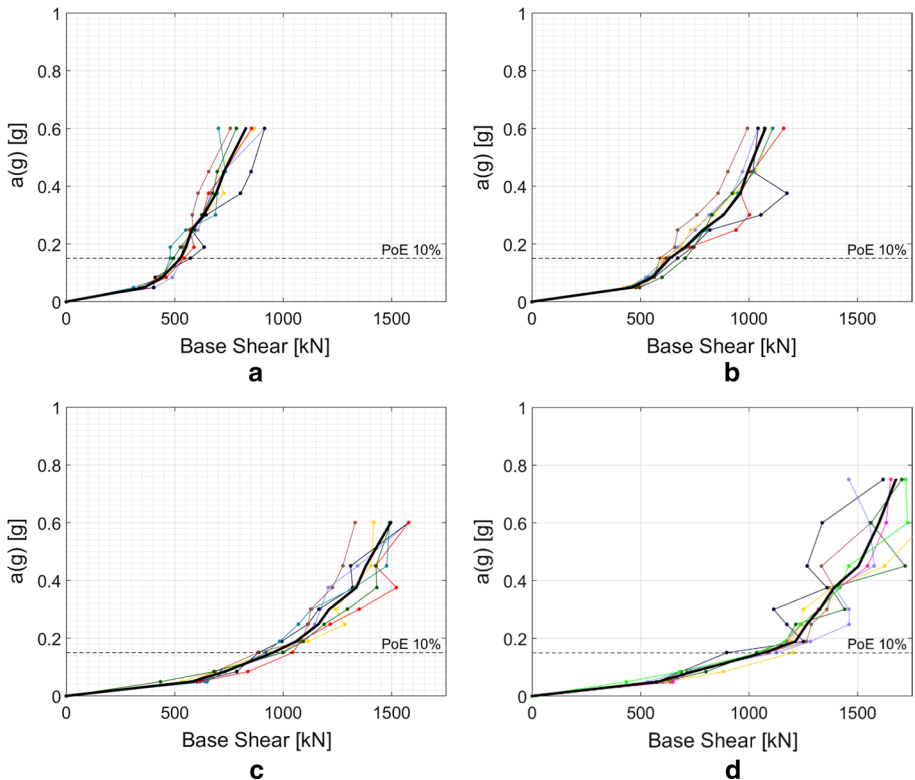
Fig. 10 Comparisons between the global base shear values (kN) and the scaled accelerations (g). **a** DCL (benchmark), **b** DCL + 1, **c** DCL + 2 and **d** DCL + 3

the probabilistic seismic hazard curve (PSH) at a site characterized by low-to-moderate seismicity (Parma-Italy). Probability of Exceedance (PoE) of these scaled accelerations are 63, 39, 10, 5, and 2%. Five extra scale factors (2.00, 2.50, 3.00, 4.00, 5.00) are defined to observe the collapse resistance of the most resistant models. Furthermore, acceleration values have been multiplied by a factor of 1.18, in order to take into account the accidental torsion that is normally not available in the 2D planar analysis.

IDA curves have been plotted recording the maximum base shear (Fig. 10), first inter-storey drifts (Fig. 11), and displacement (Fig. 12) values from a total of 280 analyses. The values are plotted against the scaled values of PGA (a_g), as shown in the vertical axis. Each time-history result is represented by a different colour, while the black curve represents the average value of all the time histories. Figure 10 shows that from DCL to DCL + 3, at each modelling improvement, the frame's global resistance and ductility increase. It can be noted that the global ductility and resistance of the DCL + 2 and DCL + 3 models are by far superior to the benchmark model, and significantly superior to the other models.

Figure 11 compares the inter-storey drift of the first-floor level and the scaled acceleration for each model. It can be observed that the benchmark model DCL, for the accelerations slightly larger than the design values, suffers first inter-storey drift ratios between 1 and 2%, which may translate into a significant damage or a first story collapse. Improvements can be observed starting from DCL + 1, which withstand accelerations much larger
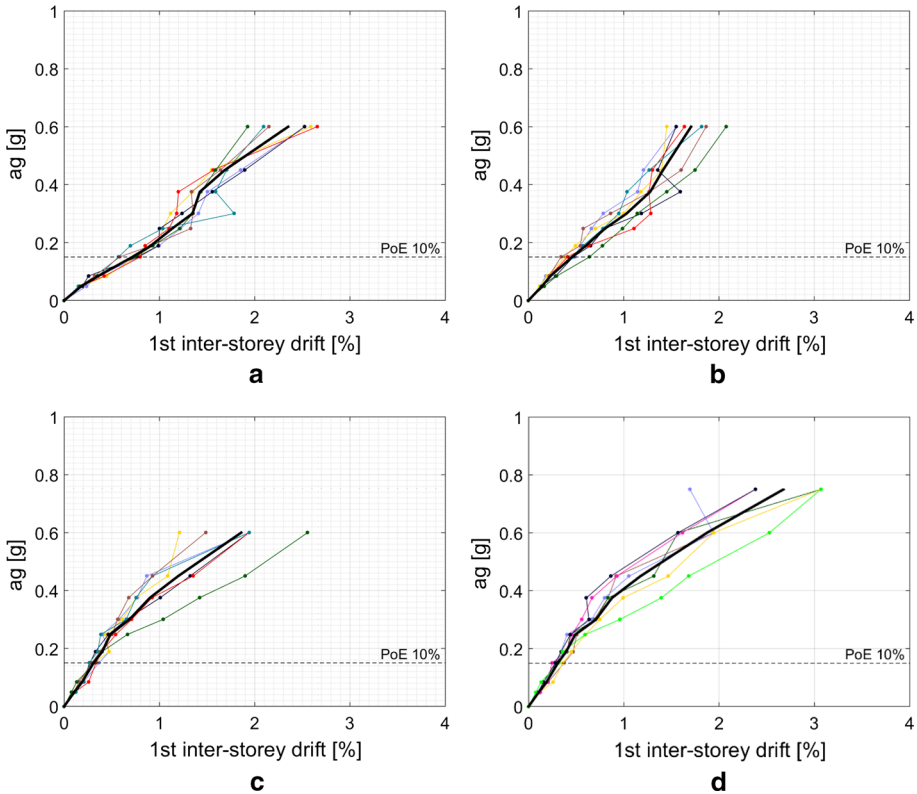
Fig. 11 Comparison between the 1st inter-storey drift (%) values and the scaled accelerations (g). **a** DCL (benchmark), **b** DCL + 1, **c** DCL + 2 and **d** DCL + 3

than the design values. Comparison of the top displacement and base shear curves also indicates the global capacity increase from DCL to DCL + 3 (Fig. 12).

Same conclusions can be drawn also from Fig. 13, which compares the average curves of all models in terms of base shear, displacement and inter-storey drift parameters. DCL + 1 and DCL + 2 have significantly higher global resistance above the design probability of exceedance. DCL + 3 has the most robust behaviour, remaining nearly elastic until large accelerations under most of the time histories, and having some ductility even at much stronger earthquakes than the design one.

Global ductility of each model (D_g) has been calculated as a proportion between the 1st inter-storey drift ratios corresponding to the collapse limit state (d_u) and the first yielding (d_y) of the structure. F_u (maximum base shear causing collapse) and d_u have been defined investigating the simulation outcomes of each model. For DCL, collapse has been defined when the first bracing joint failure has been observed. For the other models (DCL + 1, DCL + 2 and DCL + 3), collapse has been defined when the first column yielding has been observed. F_y (maximum base shear causing the first yielding) and d_y values have been calculated according to the ECCS45 (1986) procedure: the initial stiffness of the capacity curves has been estimated by the tangent slope obtained at the origin. Then, a tangent line with a slope of 10% of the initial stiffness slope on the
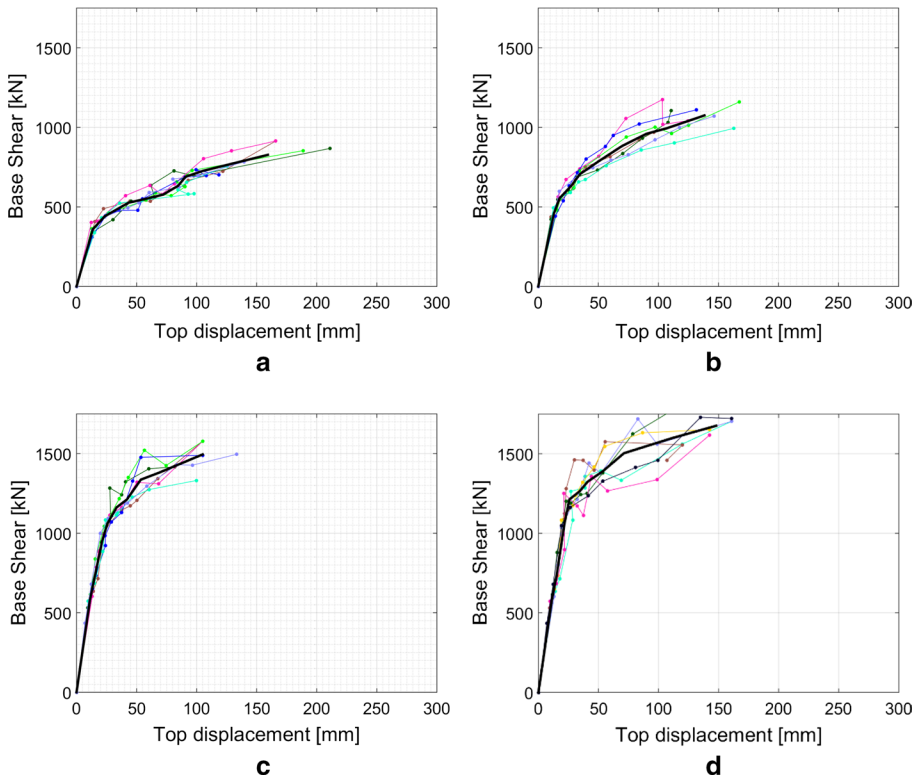
Fig. 12 Comparison between the top displacement (mm) and base shear (kN) values. **a** DCL (benchmark), **b** DCL + 1, **c** DCL + 2 and **d** DCL + 3

global force—1st inter-storey drift curves has been plotted. The intersection of the two tangent lines defines the values of d_y and F_y (Fig. 14), which are reported in Table 9.

From these observations, global performance of the case studies have been quantified with D_{inc} and $F_{u,inc}$ parameters, showing how much the global ductility and resistance of "+" models improve with respect to the benchmark (for instance, D_{inc} [DCL + 1] = D_g [DCL + 1]/D_g [DCL], $F_{u,inc}$ [DCL + 1] = F_u [DCL + 1]/F_u [DCL].)

These results are graphically presented in Fig. 15, which shows how the global behaviour improves both in terms of ductility and resistance from DCL to DCL + 3. The DCL + 3 has the best overall performance, with an increased ductility 1.9 times DCL ductility, also characterized by a relatively very large base shear reached at global collapse.

Results have been also interpreted by means of time vs 1st inter-storey drift ratio history for a single accelerogram. Figure 16 shows this comparison for the design seismic action (PGA 0.15 g) and reports the deformed shapes when the models suffer the largest 1st inter-storey drifts within their time-history. In the graphs, the 1st inter-storey drifts are shown by black curves, while the other colours refer to the inter-storey drift values of the upper floors. DCL has significantly higher 1st inter-storey drifts with respect to the other models. Although at the design situation, they are lower than the code damage limits (1%), such a
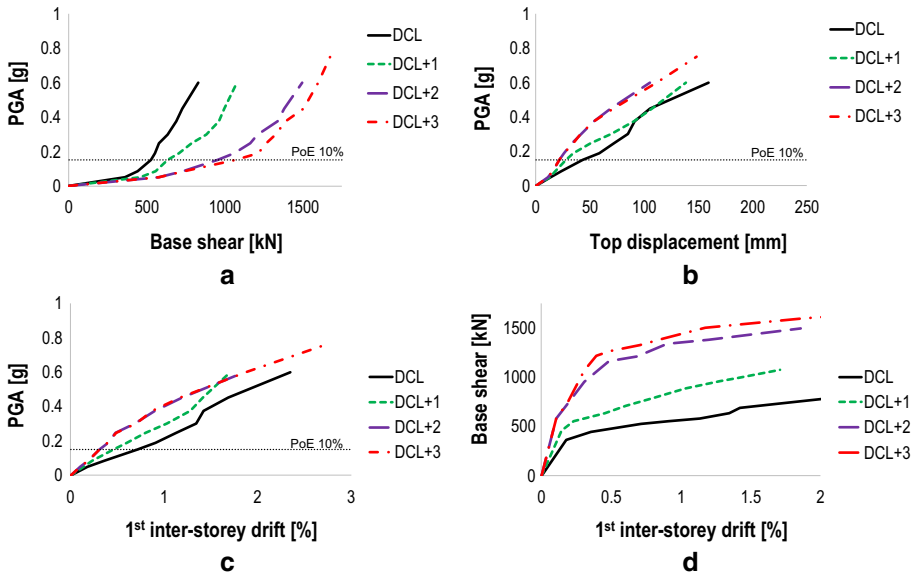
Fig. 13 Comparison of results in terms of average values. **a** Base shear (kN) versus PGA (g), **b** top displacement (mm) versus PGA (g), **c** 1st inter-storey drift (%) versus PGA (g) and **d** 1st inter-storey drift (%) versus base shear
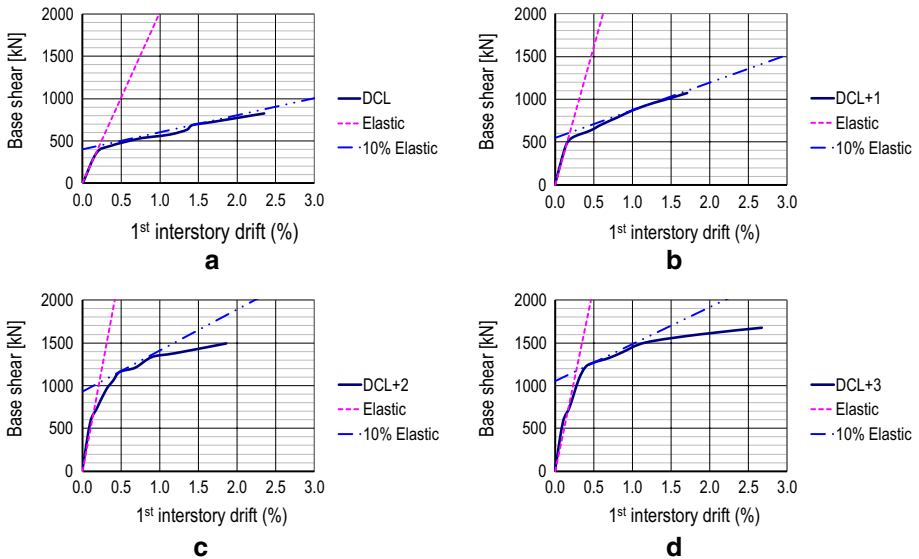

Fig. 14 Calculation of the f_y and d_y values. **a** DCL, **b** DCL + 1, **c** DCL + 2 and **d** DCL + 3

situation may indicate a "soft story" alarm for the less expected but higher accelerations. Indeed, Fig. 17 presents this risk, where the 1st inter-storey drift ratios are shown for three scaled accelerograms with PGA of 0.15 g (10% PoE), 0.189 g (5% PoE), and 0.248 g (2%

Table 9 Parameters used to quantify ductility and resistance of case studies

	d_y (%)	F_y (KN)	d_u (%)	F_u (KN)	Collapse mode	D_g (d_u/d_y)	D_{inc}	$F_{u,inc}$
DCL	0.22	449	1.13	578	Bracing joint failure	5.1	1	1
DCL+1	0.19	610	1.50	1000	Column yielding	7.9	1.5	1.7
DCL+2	0.22	1033	1.86	1495	Column yielding	8.5	1.7	2.6
DCL+3	0.27	1171	2.68	1676	Column yielding	9.9	1.9	2.9

Fig. 15 Comparison of ductility and resistance performances of different models
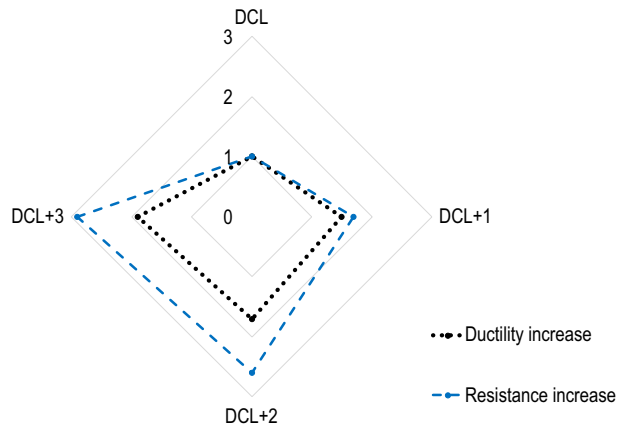
PoE), for all models. It is evident that "+" models are more resilient for higher accelerations, being DCL + 2 and DCL + 3 the more robust ones.

Figure 18 shows that, in the design situation, none of the models has a collapse risk. However, at higher acceleration values, DCL is the first one to enter in the collapse risk zone. DCL + 2 and DCL + 3 only enter the risk zone when the ground acceleration is more than two times the design value (at 0.4 g). These latter two models will reach collapse (reaching a max inter-storey drift larger than 2%), only under a PGA of 0.6 g. This comparison shows that the real ductility and resistance of a low-dissipative CBF systems can be indeed much higher with respect to their design value, when inherent benefits due to actual element and joint behaviour are exploited. Ductility and resistance can be significantly enhanced by means of a limited bracing slenderness combined with moderately ductile connections.

Conclusions can be listed as:

- A first remarkable improvement has been noted for model DCL + 1, which takes into account the frame action provided by the gusset plates.
- Setting the higher slenderness limit to λ = 2.25 (represented by model DCL + 2), a significant increase has been achieved in the global resistance and ductility.
- Although capacity design requirement was not met for the bracing joints of the model DCL + 2 (C_R ~ 0.8), a moderate global ductility was achieved. Increasing the capacity design ratio from 0.8 (DCL + 2) to 1.25 (DCL + 3), the global ductility and resistance increases were respectively 1.9 and 2.9 times the values of DCL.
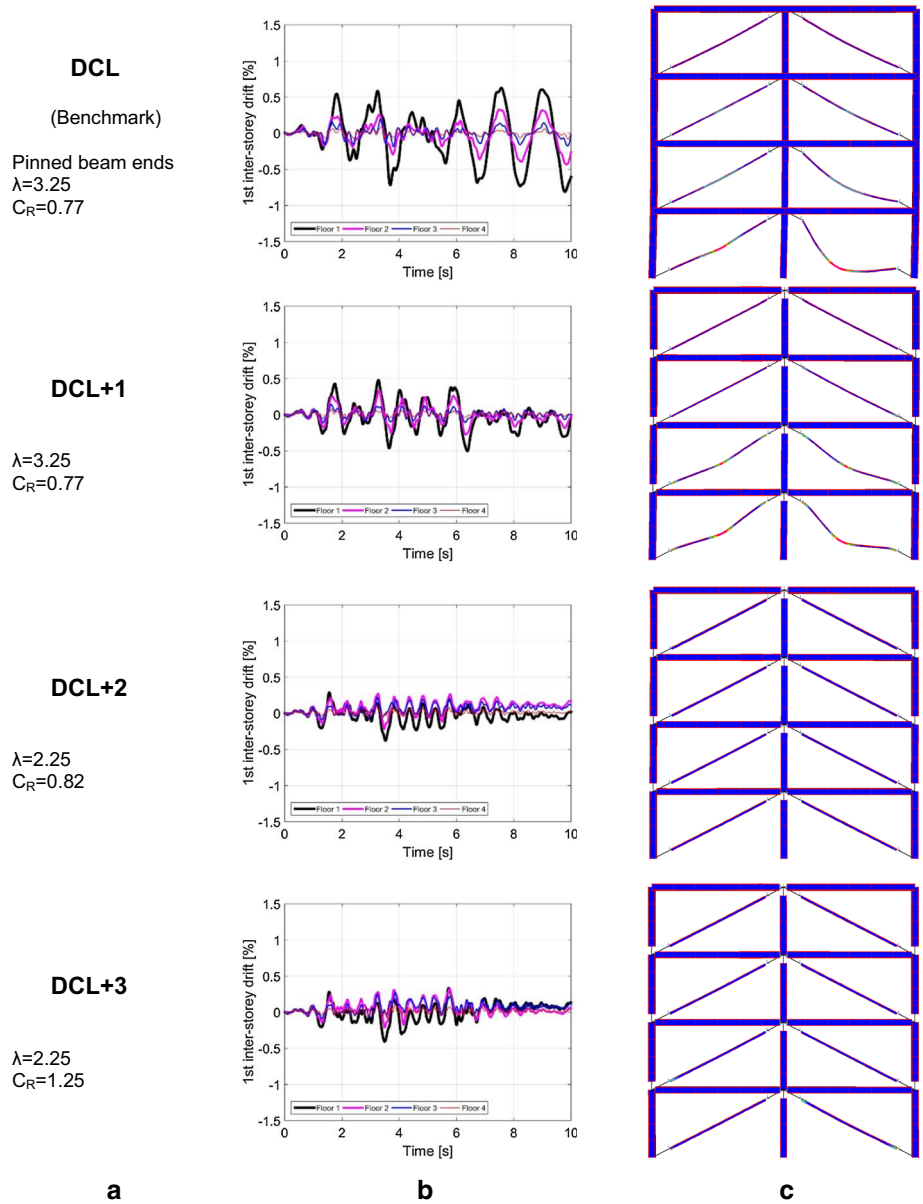
Fig. 16 Time vs 1st inter-storey drift history for ACC1 and deformed shapes during the largest inter-storey drift of each simulation. **a** Model assumptions, **b** 1st time vs inter-storey history for ACC1 (PGA: 0.15 g) and **c** relevant deformed shape

The "back-up" ductility and resistance sources of low-dissipative CBFs can be valuable in low-to-moderate seismicity, where "larger-than-design" seismic events are foreseeable. In order to achieve this, stringent requirements for high-dissipative design (DCM or DCH)
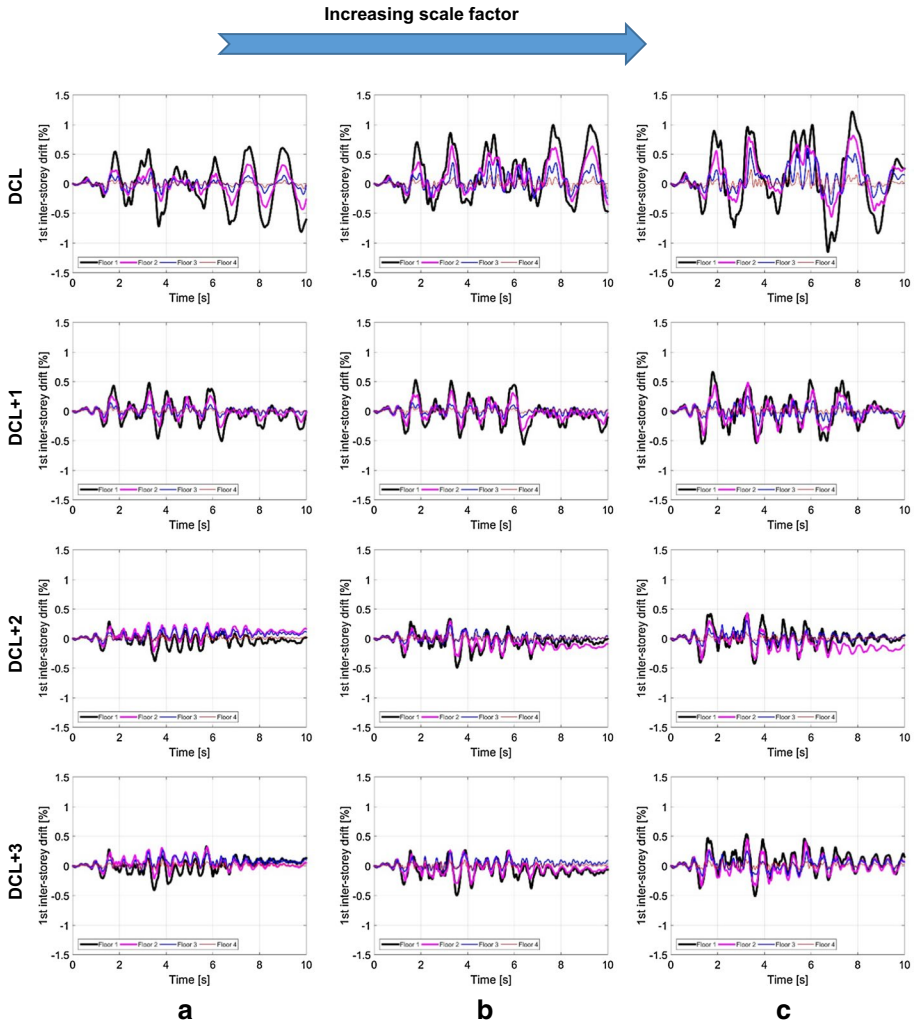
Fig. 17 Time vs 1st inter-storey drift history for ACC1 (PGA: 0.15 g, 0.189 g and 0.248 g). **a** 0.15 g (10% PoE), **b** 0.189 g (5% PoE) and **c** 0.248 g (2% PoE)

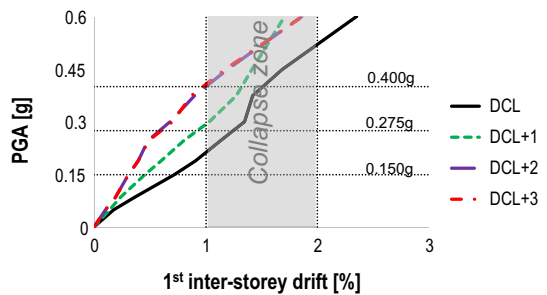**Fig. 18** Collapse risk of the case studies according to PGA

Table 10 Bracing configurations of two frame types

Fl.	DCL		DCL + 2 (DCL + slenderness limitations + Meakado rules on connections)		DCL + 3 (DCL + slenderness limitations + Capacity design of connections)		DCM	
	Bracing profiles	Bracing joint	Bracing profiles	Bracing joint	Bracing profiles	Bracing joint	Bracing profiles	Bracing joint
4	2L70x7	4M20	2L100x8	4M20	2L100x8	9M20 + extra angle	2L100x8	9M20 + extra angle
3	2L70x7	4M20	2L100x8	4M20	2L100x8	9M20 + extra angle	2L120x10	9M20 + extra angle
2	2L70x7	4M20	2L100x8	4M20	2L100x8	9M20 + extra angle	2L120x15	9M20 + extra angle
1	2L70x7	4M20	2L100x8	4M20	2L100x8	9M20 + extra angle	2L150x12	9M20 + extra angle

should not necessarily be met. The "DCL + 2" approach, combining a maximum slenderness limit of 2.25, a moderate joint ductility with capacity design ratio of at least 0.85, and a proper gusset plate design can be economically useful for the design of CBF systems in the low-to-moderate seismicity regions.

4.3 Economic considerations

For the case studies designed according to the current DCL and DCM of EN1998-1-1 (2005), and the adjusted DCL approaches (DCL + 2 and DCL + 3), steel frame costs have been compared. Table 10 shows the frame configurations originated from the four approaches. Clearly, the capacity design rules related to DCM result in larger bracing profiles and more robust connections. Except for the bracing profiles and their connections, the other frame parameters are unchanged z (column, beam profiles, their connections and the dimensions).

Table 11 reports the unit costs for steel used in the cost calculations, based on the Italian construction market within the publication year of this article. Table 12 shows the comparisons between the four building types. In the first eight rows of the table, results are shown with reference to the plane braced frame (Fig. 6b), in the last three rows, they are extended to the whole building (Fig. 6a). Assuming that the bracings influence the 4% of total structure costs (this assumption is based on the database of a steel construction company operating in Italy), DCM, DCL + 2 and DCL + 3 configuration costs are respectively 7.8%, 2.1% and 4.5% higher with respect to DCL.

5 Conclusions

This article focuses on a normative problem, which currently may cause expensive and unsafe steel structures in low-to-moderate seismicity regions. Current European building codes do not provide a clear design method in the low-to-moderate seismicity context; there are two recommended options:

1st option: Apply low-ductility concept (DCL): It does not require any specific ductility rule.
2nd option: Apply medium-ductility concept (DCM): It requires the fulfilment of all the stringent rules of the high-ductility concept (DCH), such as structural homogeneity, slenderness limits, and connection over-strength. The only difference with respect to high seismic design criteria is the allowance of a lower behaviour (q) factor.

Table 11 Unit costs of steel construction (according to Italian market)

Material cost of steel	€1.5/kg
Material cost of bolted joints	€4.5/bolt
Material cost of preloaded bolted joints	€5.6/bolt
Assembly cost of bolted joints	€3.3/bolt
Assembly cost of preloaded bolted joints	€4.3/bolt

Table 12 Cost comparisons between the four building types based on the Italian construction market within the publication year of this article

	DCL	DCL+2 (DCL+slenderness limitations+Meakado rules on connections)	DCL+3 (DCL+slenderness limitations+capacity design of connections)	DCM
Plane frame (4 floors)				
Bracing profile weight (tons)	0.55	0.92	0.92	1.63
Bracing profile cost (€)	826	1384	1384	2451
Bracing joint material cost (€)	288	358	806	806
Bracing joint assembly cost (€)	211	275	619	619
Total bracing joint cost (€)	499	634	1426	1426
Subtotal sum (€)—Bracings	1325	2017	2809	3877
Saving at fabrication phase (€)	(−) 14	(−) 23	(−) 23	(−) 0
Total sum (€)	1311	1994	2786	3877
All building				
Total sum for 4 braced frames (€)	5245	7977	11145	15507
Cost increment of bracings		+52.1%	+112.5%	+195.7%
Cost increment for steel structure		+2.1%	+4.5%	+7.8%

As a result, most of the engineers choose DCL approach because of its simplicity, and avoid complex and expensive requirements of the current DCM. However, this "simple" DCL approach disregarding any seismic requirement may lead to unsafe structures, as the nature of low-to-moderate seismicity regions is quite unpredictable. Rare but strong earthquakes are foreseeable in these areas. On the other hand, obligating engineers to apply the strict high-ductility rules seem too conservative for low-to-moderate seismicity, which would result in over-safe but uneconomic structures. This is a critical problem considering that CBF systems are some of the most common structural frame configuration choices in Europe. This article aimed to develop an "intermediate" approach, which would result in safe and economic CBF structures. The proposed approach is based on the exploitation of some natural features of CBF systems, namely:

- Frame action provided by gusset plates.
- Post-buckling strength and stiffness of the compression diagonal.
- Energy dissipation capacity of bracing joint connections.

Such phenomena are not normally taken into account for the seismic design, because their contribution remains marginal for the high seismicity demands. This paper investigated and quantified these phenomena, in order to let practising engineers exploit them in the context of low-to-moderate seismicity. The findings of this paper resulted in a final proposal of a "DCL+" approach for the design of CBF systems in low-to-moderate seismicity regions (so-called "DCL + 2" in the case study described in this paper). The additional requirements of this method with respect to current "DCL" are the following:

1. Gusset plates should be designed to remain elastic, and connected both to the beam and the column.
2. Upper limit of bracing slenderness should be kept as 2.25.
3. Bracing joints should be designed with a capacity ratio of at least 0.85, and their bolted connections should be pre-loaded (category B or C of EN1993-1-8).
4. If the above three requirements are met, a behaviour factor (q) of 2.50 can be allowed, thanks to the exploitation of the benefits of the frame action, compression diagonal, and moderate ductility of the standard preloaded bracing joints.
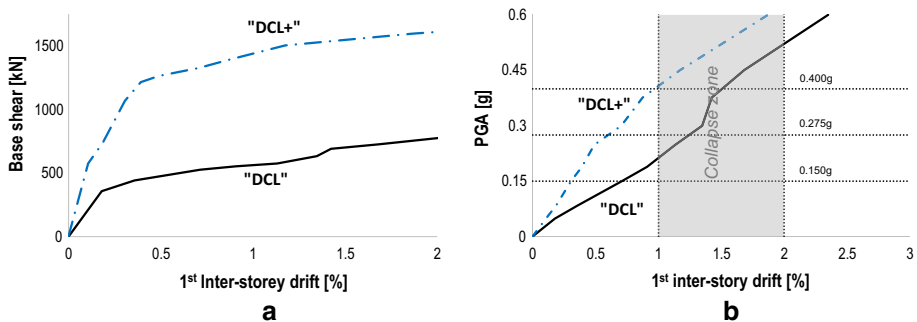

Fig. 19 Comparison between "DCL" and "DCL+" approach. **a** Global base shear vs inter-storey drift curves and **b** inter-storey drift versus scaled PGA curves

Figure 19 compares the global performance of a case study designed with current "DCL" and new "DCL+" approaches by means of average IDA curves. The improvement in the global behaviour and decrease of the collapse risk in case of "DCL+" method can be noted. The structure designed according to "DCL+" is much more robust and ductile, and enters the collapse zone at much higher accelerations. Such improvement in the structural behaviour corresponds to a cost increment of 2.1% for the steel structure budget.

In the literature, the availability of the full-scale experimental and numerical studies of ordinary CBF structures (designed without seismic provisions) is limited. This article presented one of them, with the aim of contributing to the development of the future guidelines regarding the low-to-moderate seismicity design. There are several points that can be improved to extend its findings. It is also worthwhile to study new parameters that can further optimize the behaviour of CBFs in low-to-moderate seismicity regions. Therefore, the following future research needs can be identified:

- A parametric numerical analysis is needed to understand the effect of several parameters which had to be kept constant in this study: gusset plate geometry and thickness, changing column and beam profile cross-sections, different span lengths and bracing inclinations, different bracing profile types (closed sections, or other type of open sections such as UPN), connection typologies and configurations.
- Experiments should be performed with different gusset plate connection types, since this is a very promising source of CBF ductility and resistance.
- The effect of vertical loading on the columns should be investigated by means of numerical or experimental studies to observe second-order effects on the global performance of CBFs.
- Numerical and experimental investigations are needed to discover other potential secondary resources of CBFs, such as: composite action provided by the concrete slab at the connection zone, moderately ductile column bases, out of plane plastic deformation of gusset plates and non-structural elements.
- Benefits of replaceable dissipative connections and devices should be investigated in the context of low-to-moderate seismicity.
- The implementation of the design recommendations proposed in this article into normative documents or seismic regulations requires further validation in order to assess their reliability. This can be done by means of a real risk analysis including both the variability of the seismic action (considering natural time-histories) and the variability of the material properties, applied to a larger set of archetype structures.
- Additional examples may be studied to investigate deeply the practical consequences of the suggested design rules.
- To prove the safety of the upper slenderness limit value stated in this article, extra tests and analysis should be performed considering the impact forces induced by the re-tensioning of buckled diagonal braces.

References

Aboosaber M, Hines EM (2011) Modeling reserve system performance for low-ductility braced frames, Interim report submitted to: the American Institute of Steel Construction under the Contract: "Moderate ductility dual systems and reserve capacity" Tufts University, Report no. TUSSR-2011/1, July 2011

American Institute of Steel Construction (2010) Seismic Provisions for Structural Steel Buildings, ANSI/AISC 341-05, March 9, 2005, incl. Supplement No. 1

Bradley CR, Fahnestock LA, Hines EM, Sizemore JG (2017) Full-scale cyclic testing of low-ductility concentrically braced frames. J Struct Eng 143(6). https://doi.org/10.1061/(ASCE)ST.1943-541X.0001760

Brandonisio G, Toreno M, Grande E, Mele E, De Luca A (2012) Seismic design of concentric braced frames. J Constr Steel Res 78:22–37. https://doi.org/10.1016/j.jcsr.2012.06.003

Costanzo S, D'Aniello M, Landolfo R (2017) Seismic design criteria for Chevron CBFs: European vs North American codes (part-1). J Constr Steel Res 135:83–96. https://doi.org/10.1016/j.jcsr.2017.04.018

Degée H, Henriques J, Vleminckx L, Denoel V, Hoffmeister B, Wieschollek M, Castiglioni CA, Kanyilmaz A, Martin PO, Rodier A, Couchaux M, Calderon I, Aramburu A, Galazzi A, Cornil A, Duchene Y, Radu J (2018) Design of steel and composite structures with limited ductility requirements for optimized performances in moderate earthquake areas, Final report MEAKADO RFSR-CT-2013-00022. European Comission, Research Fund for Coal and Steel

ECCS45 Technical Committee 1—Structural Safety and Loadings Technical Working Group 1.3—Seismic Design (1986) Recommended testing procedure for assessing the behaviour of structural steel elements under cyclic loads

Elghazouli A (2009) Assessment of European seismic design procedures for steel framed structures. Bull Earthq Eng 8:65–89. https://doi.org/10.1007/s10518-009-9125-6

EN 1090-2 (2011) Execution of steel structures and aluminium structures part 2: technical requirements for steel structures

EN 1993-1-1 (2005) European standard. Eurocode 3: design of steel structures—Part 1–1: general rules and rules for buildings

EN1998-1-1 (2005) Eurocode 8—design of structures for earthquake resistance-Part 1: general rules, seismic actions and rules for buildings

Eurocode 3: design of steel structures - Part 1–8: design of joints, 2005

Gioncu V, Mazzolani F (2014) Seismic design of steel structures. CRC Press, Taylor & Francis Group, Boca Raton

Kanyilmaz A (2015a) Validation of fiber-based distributed plasticity approach for steel bracing models. Civil Eng J 1:1–13

Kanyilmaz A (2015b) Inelastic cyclic numerical analysis of steel struts using distributed plasticity approach. In: COMPDYN 2015—5th ECCOMAS thematic conference on computational methods in structural dynamics and earthquake engineering, National Technical University of Athens, pp 3663–3674

Kanyilmaz A (2017a) Secondary frame action in concentrically braced frames designed for moderate seismicity: a full scale experimental study. Bull Earthq Eng 15:2101–2127. https://doi.org/10.1007/s10518-016-0054-x

Kanyilmaz A (2017b) Role of compression diagonals in concentrically braced frames in moderate seismicity: a full scale experimental study. J Constr Steel Res 133:1–18. https://doi.org/10.1016/j.jcsr.2017.01.023

Kanyilmaz A (2018) Moderate ductility of the bracing joints with preloaded bolts. Bull Earthq Eng 16:503–527. https://doi.org/10.1007/s10518-017-0208-5

Kanyilmaz A, Castiglioni CA (2015) Performance of multi-storey composite steel-concrete frames with dissipative fuse devices. In: COMPDYN 2015—5th ECCOMAS thematic conference on computational methods in structural dynamics and earthquake engineering, pp 334–348

Kanyilmaz A, Castiglioni CA, Degèe H, Martin P (2015) A preliminary assessment of slenderness and over-strength homogenity criteria used in the design of concentrically braced steel frames in moderate seismicity. In: COMPDYN 2015—5th ECCOMAS thematic conference on computational methods in structural dynamics and earthquake engineering, pp 3599–609

Kazemzadeh Azad S, Topkaya C, Astaneh-Asl A (2017) Seismic behavior of concentrically braced frames designed to AISC341 and EC8 provisions. J Constr Steel Res 133:383–404. https://doi.org/10.1016/j.jcsr.2017.02.026

Kelly DJ, Zona JJ (2006) Design tips for steel in low or moderate seismicity regions. Mod Steel Constr 46(2):50–56

Landolfo R (2012) Assessment of EC8 provisions for seismic design of steel structures, 1st edn. ECCS TC13 Seismic Design, ECCS - European Convention for Constructional Steelwork

Longo A, Montuori R, Piluso V (2008) Failure mode control of X-braced frames under seismic actions. J Earthq Eng 12(5):728–759. https://doi.org/10.1080/13632460701572955

Marino EM, Nakashima M, Mosalam KM (2005) Comparison of European and Japanese seismic design of steel building structures. Eng Struct 27:827–840. https://doi.org/10.1016/j.engstruct.2005.01.004

Martin PO, Rodier A, Couchaux M, Kanyilmaz A, Degee H (2017) Assessment of the ductile behaviour of CBF structures considering energy dissipation in bolted joints. In: EUROSTEEL 2017, September 13–15, Ernst & Sohn, Copenhagen, Denmark

Mayer Rosa D (1993) Towards uniform earthquake hazard assessment. Analisi Di Geofisica XXXVI:93–102

Murty CVR, Malik JN (2008) Challenges of low-to-moderate seismicity in India. Electron J Struct Eng 8:77–87

Nordenson GJP, Bell GR (2000) Seismic design requirements for regions of moderate seismicity. Earthq Spectra 16:205–225. https://doi.org/10.1193/1.1586091

NTC 2008 (2008) Decreto Ministeriale 14/1/2008 - norme tecniche per le costruzioni. Ministry of Infrastructures and Transportations, Italy

Pinto PE (2000) Design for low/moderate seismic risk. Bull N Z Soc Earthq Eng 33:303–324

Sabelli R (2001) Research on improving the design and analysis of earthquake-resistant steel-braced frames. NEHRP professional fellowship report EERI, pp 1–142

Shen J, Seker O, Akbas B, Seker P, Momenzadeh S, Faytarouni M (2017) Seismic performance of concentrically braced frames with and without brace buckling. Eng Struct 141:461–481. https://doi.org/10.1016/j.engstruct.2017.03.043

Stoakes CD (2012) Beam-column connection flexural behavior and seismic collapse performance of concentrically braced frames. Ph.D. Thesis, University of Illinois at Urbana-Champaign

Tremblay R (2002) Inelastic seismic response of steel bracing members. J Constr Steel Res 58:665–701. https://doi.org/10.1016/S0143-974X(01)00104-3

Tremblay R, Archambault M-H, Filiatrault A (2003) Seismic response of concentrically braced steel frames made with rectangular hollow bracing members. J Struct Eng 129:1626–1636. https://doi.org/10.1061/(ASCE)0733-9445(2003)129:12(1626)

Uriz P, Mahin S (2008) Toward earthquake-resistant design of concentrically braced steel-frame structures, PEER report 2008/08 Pacific Earthquake Engineering Research Center College of Engineering University of California, Berkeley

Vamvatsikos D, Cornell CA (2002) Incremental dynamic analysis. Earthq Eng Struct Dyn 514:491–514. https://doi.org/10.1002/eqe.141

Strand7 Pty Ltd. (2014) http://www.strand7.com/